PERGAMON

Journal of Atmospheric and Solar-Terrestrial Physics 64 (2002) 115–124

Journal of ATMOSPHERIC AND SOLAR-TERRESTRIAL PHYSICS

www.elsevier.com/locate/jastp

A new framework for studying the relationship of aurora and plasma sheet dynamics

G.K. Parks[a,b,*], L.J. Chen[a], M. Fillingim[a], R.P. Lin[b], D. Larson[b], M. McCarthy[a]

[a] *Geophysics Program, University of Washington, Seattle, WA 98195, USA*
[b] *Space Sciences Laboratory, University of California, Berkeley, CA 94720, USA*

Received 7 November 2000; received in revised form 5 March 2001; accepted 5 March 2001

Abstract

Auroras have been extensively studied using images obtained by space-borne experiments. We use global UVI images obtained from Polar and simultaneous plasma data obtained by the 3D instrument on Wind from the near-earth plasma sheet to study the dynamics of auroras with different size and intensity. Unstable phase space ion distributions are detected in the plasma sheet under diverse geomagnetic and solar wind IMF conditions (positive and negative B_z) and at all phases of a substorm. These results indicate that plasma instability processes with different disturbance levels operate in the plasma sheet and produce a continuum of auroral size and intensity. The criteria for triggering an instability are dependent on the local properties of the plasma distributions. These observations suggest a new framework to integrate previous and current results and a new way to examine the causal relationships of auroral and plasma sheet dynamics.

Keywords: Aurora dynamics; Plasma sheet dynamics

1. Introduction

A fundamentally important unsolved problem in space plasma physics deals with how energy transported in the plasma sheet is dissipated in magnetospheric substorms. Substorms accelerate particles over a wide pitch-angle range including the loss cone from which electrons precipitate into the ionosphere and produce auroras. In studying the relationship between the aurora and plasma sheet dynamics, it is important to note that auroras have a continuum of intensities and sizes. They include the very weak pseudo-breakup auroras that cover a tiny fraction of the auroral oval to expansive auroras that cover the entire night side auroral oval.

The term pseudo-breakup aurora describes the disruption of an arc other than the equatorward most arc (Elvey, 1957). This is in contrast to the behavior of expansive type auroras whose disruption starts with the equatorward most arc (Akasofu, 1964). A pseudo-breakup aurora appears "different" because it lacks the expansion phase of a "normal" auroral substorm. However, recent studies of ion dynamics in the plasma sheet during pseudo-breakup and expansive auroras indicate that nearly identical physics is involved (Chen et al., 2000a; Fillingim et al., 2000). High-speed mean velocities ($\langle \mathbf{v} \rangle = \int \mathbf{v} f(\mathbf{r}, \mathbf{v}) \, \mathrm{d}^3 v$) exceeding 400 km/s are observed to occur during both of these forms of auroras. These high $\langle \mathbf{v} \rangle$s come from phase space distributions that include non-gyrotropic beams, involve freshly accelerated energetic ions from a few keV to MeV energies, and large-amplitude magnetic field fluctuations (all three components) close to the local cyclotron frequency. These features are observed during both northward and southward B_z components of the interplanetary magnetic field (IMF) and at all levels of the geomagnetic activity and phases of a substorm, not just during the onset phase but also the recovery phase.

This article will review and discuss these recent findings that provide new insights into the relationship of the aurora

* Corresponding author. Space Sciences Laboratory, University of California, Berkeley, CA 94720, USA. Fax: +1-510-643-8302.
E-mail address: parks@ssl.berkeley.edu (G.K. Parks).

1364-6826/02/$ – see front matter
PII: S 1364-6826(01)00078-5

and plasma processes that occur in the plasma sheet. On the basis of these observations, we suggest that the dynamics in the plasma sheet, like the aurora, operate in a continuum of disturbance levels. These disturbances, produced by instabilities in the plasma sheet, accelerate and inject particles over a broad range of pitch-angles. The unstable electron distributions radiate auroral kilometric radiation and precipitate energetic electrons into the ionosphere and produce the aurora. The instability can be small and localized or global involving the entire geomagnetic tail and produces a continuum of auroral precipitation size and intensity. The actual plasma instability process is not yet identified but observed variations of the magnetic field are large, $\Delta B/B > 1$, indicating the process is nonlinear. Our observations further indicate the conditions for triggering an instability are dependent primarily on the local properties of the plasma distributions in the plasma sheet.

2. Aurora and plasma sheet dynamics

Fig. 1 shows a sequence of auroral images from July 26, 1997 (pseudo-breakup events) and March 27, 1996 (expansive aurora) displayed as a function of the magnetic latitude (MLAT) and magnetic local time (MLT). These images come from the UVI camera on Polar operating in the mode that detected Lyman–Birge–Hopfield (LBH) emissions in the wavelength band, 160–180 nm (Torr et al., 1995). The brightness in the LBH wavelength range is directly proportional to the energy deposition rate (power) into the ionosphere carried by precipitating electrons. The angular resolution of the UVI camera is 8° and the pixel size is $\approx 0.04^\circ$ and projects to a $\approx 40 \times 40$ km^2 area at 100 km altitude. (These images have not been corrected for the platform wobble of $\approx 0.4^\circ$.)

More than 10 pseudo-breakup events occurred during the time interval 0400–0700 UT on July 26, 1997 (Fillingim et al., 2000). A sequence of images showing the development of a pseudo-breakup aurora is displayed in the top two rows. The start time of each image is shown on the top right and each image here represents photon counts accumulated over 37 s. As noted above, a pseudo-breakup aurora is associated with electron precipitation into a small region of space and lasts typically for a few minutes. On July 26, 1997 the B_z component of the IMF was mostly northward, a few nT (not shown). The pseudo-breakup auroras are easily identified during relatively quiet solar wind conditions.

The bottom two rows show a sequence of images illustrating the development of an expansive aurora. On March 27, 1996, between 0900 and 1500 UT, two major auroral expansions occurred. Ground-based magnetometers identified the first onset at ≈0943 UT and the second at ≈1425 UT (we use ground-based data to identify the onsets because the UVI had data gaps). Two smaller expansions also occurred around ≈1301 and 1408 UT. These substorm events have been studied by Angelopoulos et al. (1997) and Chen et al. (2000a). The image sequence shown come from the 1425 UT substorm. The global images cannot resolve the individual arcs, but a clear expansion onset can be seen in the image taken at 1408:26 UT. Subsequently, the aurora expanded in both latitude and longitude and covered a large fraction of the night side (see image taken at 1437:52 UT). The solar wind during 0900 to 1500 UT was fairly disturbed and the B_z component of the IMF was predominantly in the southward direction.

Let us now examine the plasma data obtained by the Wind experiments in the near-earth plasma sheet during these auroras. Wind measures 3D-particle distributions of electrons and ions with energies a few eV to several MeV (Lin et al., 1995). Fig. 2 shows keograms of the auroras obtained around local midnight from July 26, 1997 (top left panel) and March 27, 1996 (top right panel). Subsequent panels show the total power deposited in the aurora by precipitating electrons, magnetic field variations measured by Wind in the plasma sheet, three components of the mean velocities $\langle \mathbf{v} \rangle$ in GSM coordinate frame, mean velocities relative to the direction of the local magnetic field, and ion fluxes in four differential energy channels. The lines drawn through the keograms show the predicted foot-prints of Wind projected to ionospheric heights using the Tsyganenko 89 model (Tsyganenko, 1989). Note that the Wind footprint on July 26, 1997 overlapped the centers of the pseudo-breakup auroras for nearly the entire interval whereas on March 27, 1996 the overlap occurred in the region of the northern parts of the expansive aurora. On July 26, 1997, Wind was at a distance of $\approx 11 R_E$ close to the magnetic equator ($|Z_{GSM}| \langle 1 R_E$) and it moved from 21 to 00 MLT sector during the interval 0400–0700 UT. On March 26, 1996, Wind was in the dusk sector at a radial distance of $\approx 19 R_E$ at 1030 UT and $\approx 17 R_E$ at 1430 UT. The Z_{GSM} position at 0830 UT was $\approx 2 R_E$ and at 10 UT, $\approx 1 R_E$.

The keograms show that pseudo-breakup auroras have small expansions and the power deposited is ≈10–15 GW, which is less than the typical 30–100 GW deposited in an expansive aurora. Another prominent feature shown is that each auroral event (both pseudo-breakup and expansive auroras) is accompanied by an increase of the B_z component in the plasma sheet, but note that this is not the usual "dipolarization" since high-frequency variations accompany all magnetic components, B_x, B_y, and B_z. The magnetic variations reach the local ion cyclotron period. The average magnetic field intensity is 10 nT but the amplitudes of the varying magnetic field reach values as large as ≈30 nT. Thus, $\Delta B/B > 1$, suggesting the responsible processes involve nonlinear effects. Ground-based micropulsation data show occurrence of Pi-2 pulsations with each of these pseudo-breakup auroras.

Important emphasis has been given in plasma sheet studies to the high values of $\langle \mathbf{v} \rangle$ that are associated with ion distributions (Baumjohann et al., 1990; Angelopoulos et al., 1997; Fairfield et al., 1999). These $\langle \mathbf{v} \rangle$s are typically a few hundred km/s but can reach as high as ≈800 km/s. In

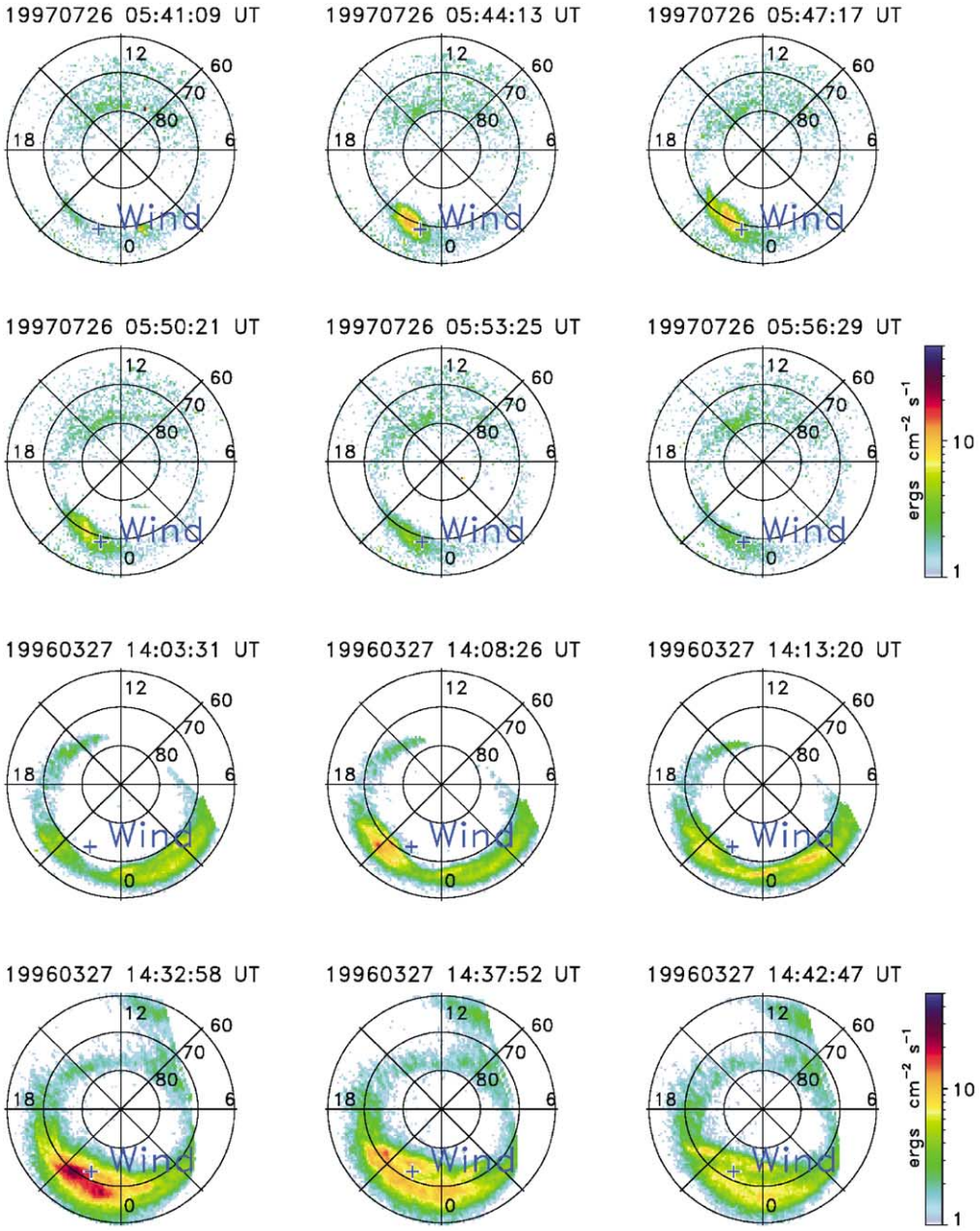

Fig. 1. Examples of global UVI images of pseudo-breakup (top two rows) and expansive auroras. Each image represents photons averaged over 37 s. The active precipitation region of pseudo-breakup aurora covers a relatively small region compared to the expansive aurora. The footprint of Wind s/c is indicated on each image.

the events we are studying, nearly every episode of high $\langle \mathbf{v} \rangle$ values in the left panel of Fig. 3 is associated with a pseudo-breakup aurora. Note that the maximum velocity attained is correlated well with the amplitude of magnetic field variations but not with the intensity of the aurora. For example, while the 0600 UT aurora is accompanied by a large value of $\langle \mathbf{v} \rangle$, smaller events around 0400 UT are also accompanied by equally large $\langle \mathbf{v} \rangle$s. Generally, the $\langle \mathbf{v} \rangle$s are predominantly along GSM X-direction but significant $\langle \mathbf{v} \rangle$s occur in the other directions. Transforming the $\langle \mathbf{v} \rangle$s into a magnetic frame of reference shows they have both parallel and perpendicular components (fifth panel). The parallel $\langle \mathbf{v} \rangle$s are directed along $\mathbf{B}$ that has a component pointing in the earthward direction.

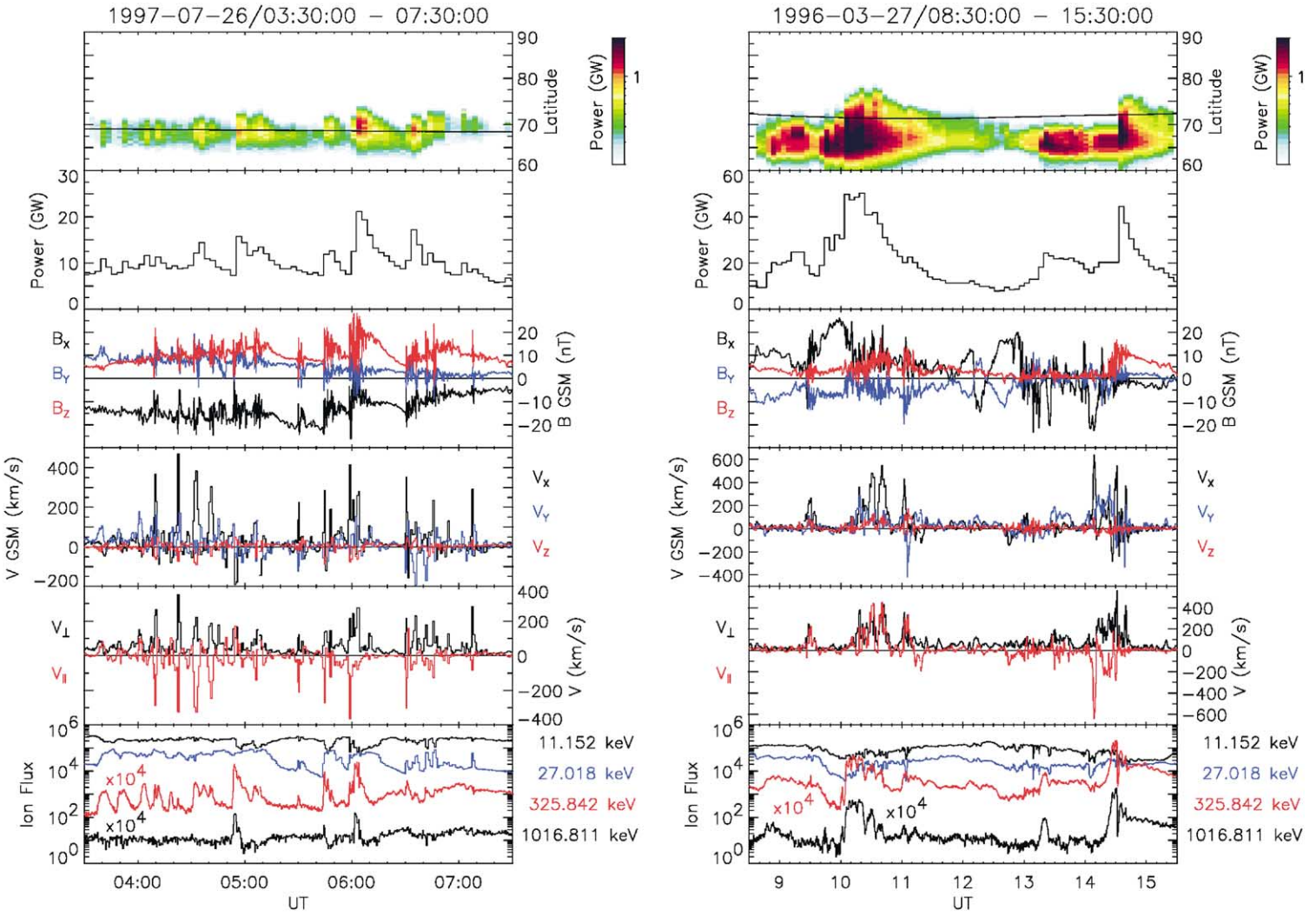

Fig. 2. The top panels show keograms of the pseudo-breakup and expansive auroras. These keograms are constructed from intensity of light at magnetic local midnight ±1 hour. The panels below them show the total dissipated aurora power, magnetic field measured by the Wind spacecraft in the plasma sheet, velocity moments of the ion distribution function measured by the 3D instrument on Wind, the velocity moments relative to the two principle directions of the magnetic field, and differential fluxes from selected ion detectors.

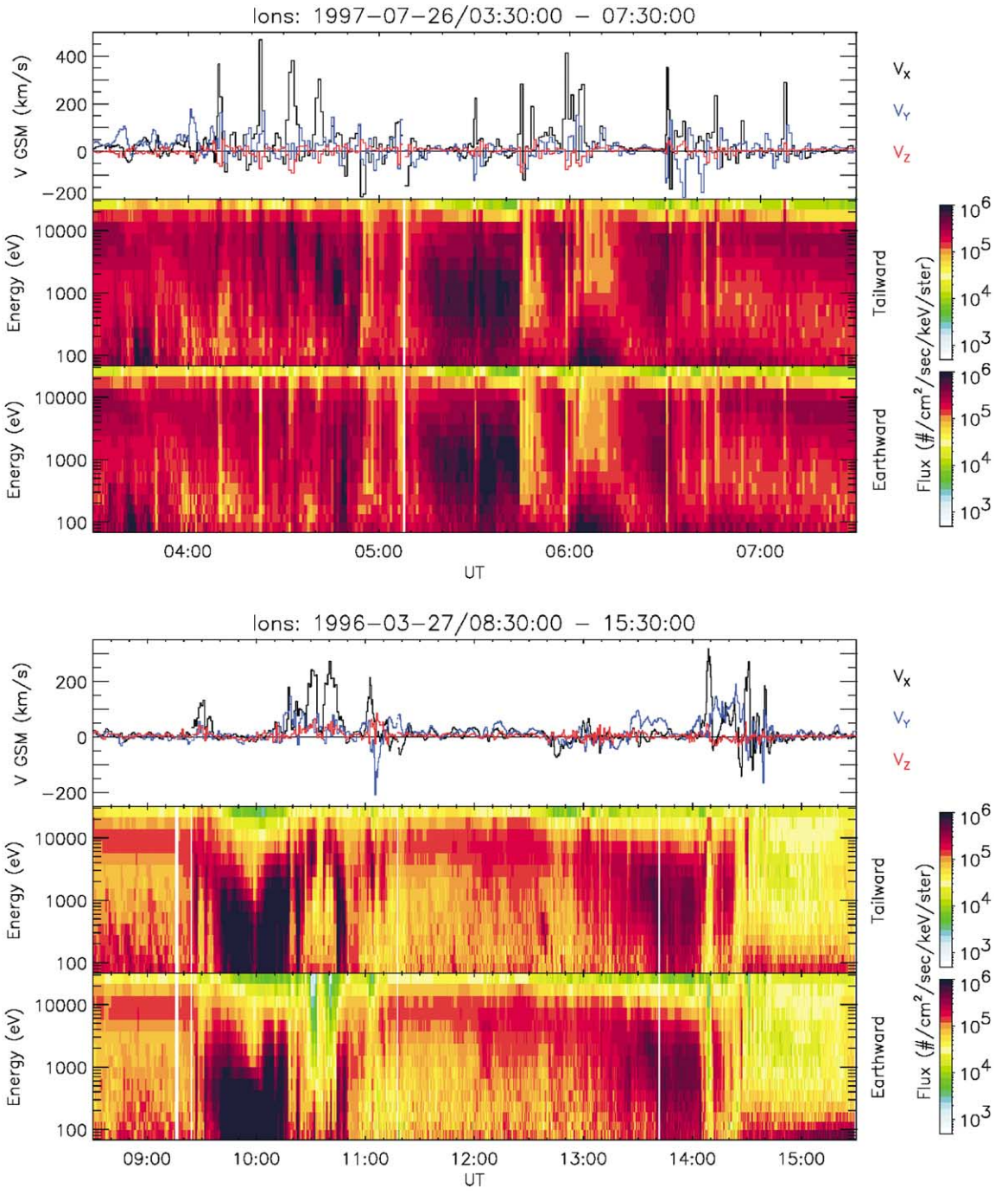

Fig. 3. Energy spectrograms of earthward and tailward travelling ions observed in the plasma sheet during the pseudo-breakup and expansive auroras. The velocity moment plots are repeated so that the spectrogram features can be correlated to the large mean velocities. PESA-H stands for Proton ElectroStatic Analyzer-High geometry instrument.

The relationship between the occurrence of high $\langle \mathbf{v} \rangle$s and the expansive aurora is more complicated. Similar to the pseudo-breakup auroras, the large $\langle \mathbf{v} \rangle$ events during expansive auroras are also accompanied by large-amplitude magnetic fluctuations. Note again that the magnetic variations occur in all three components and they are not the usual

dipolarization associated with only the B_z component. The high $\langle \mathbf{v} \rangle$s occur throughout the substorm period: at the expansion onset (Fairfield et al., 1999), as well as during the recovery phase when the aurora is fading (Chen et al., 2000a). On March 27, 1996 Wind did not detect a large $\langle \mathbf{v} \rangle$ during the first onset at ≈0943 UT. The absence of large $\langle \mathbf{v} \rangle$ can be attributed to the fact that footprint of Wind was to the north and did not overlap the expansion region. Subsequently, the substorm expanded northward, and when the northern boundary crossed the Wind footprint at ≈1010 UT, large $\langle \mathbf{v} \rangle$s began to appear. A series of five to six large bursts of $\langle \mathbf{v} \rangle$s was detected during the next hour covering the recovery phase. These events were accompanied by the intensification of a small part of the existing active aurora that covered the larger area of the night side auroral oval. The correlated behavior between the occurrence of large $\langle \mathbf{v} \rangle$s and auroral brightening observed here is nearly identical for both pseudo-breakup and expansive auroras. In both cases, plasma sheet dynamics responsible for the large $\langle \mathbf{v} \rangle$ precipitates energetic electrons with varying precipitation intensities producing a range of auroral sizes and intensities.

Two more expansions occurred at ≈1315 and ≈1425 UT. Wind did not detect large $\langle \mathbf{v} \rangle$ with the 1315 UT onset, which did not expand far enough northward for the spacecraft and the aurora to be conjugate. The small expansion at 1408 UT was associated with $\langle \mathbf{v} \rangle \approx 600$ km/s in the earthward direction. Several large $\langle \mathbf{v} \rangle$s were subsequently observed from ≈1410 to 1425 UT until the major 1425 UT onset. The 1425 UT onset was very rapid reaching the Wind footprint within 1 min and Wind detected a large $\langle \mathbf{v} \rangle$ but due to data gap, first UVI image coincides with Wind foot-print at 1432 UT. Most of the large $\langle \mathbf{v} \rangle$s were accompanied by brightening of some part of the active aurora.

But not all brightenings of the aurora in pseudo-breakup and expansive auroral events are associated with large $\langle \mathbf{v} \rangle$s and not all large $\langle \mathbf{v} \rangle$s are associated with the brightening of the aurora (Fillingim et al., 2000). For example, individual images of aurora show limited regions of the auroral oval brightened at ≈1442 UT on March 27, 1996 but no large $\langle \mathbf{v} \rangle$ was observed. Also, the aurora brightened at ≈1301 UT, again without the large $\langle \mathbf{v} \rangle$. The absence of large $\langle \mathbf{v} \rangle$ when the aurora brightens can be explained by invoking that Wind was not on the magnetic flux that connected to the aurora. This result also implies that the activity in the plasma sheet occurs in a limited region. At 0420 and 0530 UT, large $\langle \mathbf{v} \rangle$s were observed but the aurora did not brighten much. The weak auroral brightening or absence of brightening when large $\langle \mathbf{v} \rangle$ is observed indicates that the plasma sheet dynamics do not always precipitate sufficient number of energetic electrons to cause auroras.

The bottom panel shows enhanced ion fluxes at energies of several hundred kev and one MeV associated with both types of aurora. The correlated MeV ion increases and large $\langle \mathbf{v} \rangle$ events are observed when the aurora is brightening and when the Wind spacecraft maps to the region of electron precipitation. Since the auroral brightening is a temporal variation, we suggest that both large $\langle \mathbf{v} \rangle$ and the increase of MeV ions are also temporal (we realize a single-point measurement cannot distinguish absolutely spatial from temporal effects). We then deduce that the plasma mechanism that produces the large $\langle \mathbf{v} \rangle$ events also accelerates ions to MeV energies. Note that particle acceleration here occurs regardless of the size and intensity of auroras, in small pseudo-breakup events as well as in global expansive auroras. Energy spectra of these events can be found in Chen et al. (2000a) and Fillingim et al. (2001a).

We now examine energy spectrograms of the particle data to learn more about the origin of the large $\langle \mathbf{v} \rangle$s. Fig. 3 shows the $\langle \mathbf{v} \rangle$s and the energy spectrograms of earthward and tailward travelling ions with energies from ≈70 to 27 keV for the events shown in Fig. 2. The color bar on the right shows the values of the ion number flux. The largest mean velocities are in the V_x component, but it is important to note that significant V_y and V_z are also detected, albeit with smaller velocities. Each increase of $\langle \mathbf{v} \rangle$ is associated with the increases of > 10 keV earthward going fluxes which extend up to the highest energy channels of our detector (≈27 keV). At the same time, tailward going fluxes decrease from the highest energy channel down to a few keV. This shows the ions have directional dependence with a large gradient in the tailward direction. This kind of behavior is common to both intervals of pseudo-breakup and expansive auroras. The combination of the increase and decrease of high-energy ions is the main cause of the large $\langle \mathbf{v} \rangle$s.

The spectrograms show other interesting features. For example, low energy ions (≈100 eV) are often present in the plasma sheet in addition to the more energetic ions (≈1 keV). Also, more low energy ions tend to travel in the tailward direction, as seen for example at ≈1500 UT of the bottom panel. The plasma sheet ion population is often made up of multiple populations from different sources (Chen et al., 2000b).

We next examine the parent distribution function of ions from which the mean $\langle \mathbf{v} \rangle$s are derived. Fig. 4 shows, in the spacecraft frame, 2D slices of 3D distributions along the plane whose normal is defined by $\mathbf{B} \times \mathbf{V}$, where $\mathbf{V}$ is the mean velocity, with $\mathbf{B}/|\mathbf{B}|$ along the X-axis and $\mathbf{V}_\perp/|\mathbf{V}_\perp|$ along the Y-axis. The curves are isocontours of the phase space density in ($V_{||}$, $V_\perp$) space. The corresponding 1D cuts in the directions parallel and perpendicular to the magnetic field are also shown (the solid line represents the instrument background level). These plots include information on magnetic elevation angle (top left), azimuth (top right) and magnitude of the magnetic field (bottom right). The first and third rows show examples during one of the pseudo-breakup and expansive auroras. The distributions in the first column come from a time period just before the high $\langle \mathbf{v} \rangle$ was observed and the distributions in the middle and right columns come during the pseudo-breakup and expansive auroras. These distributions were constructed from

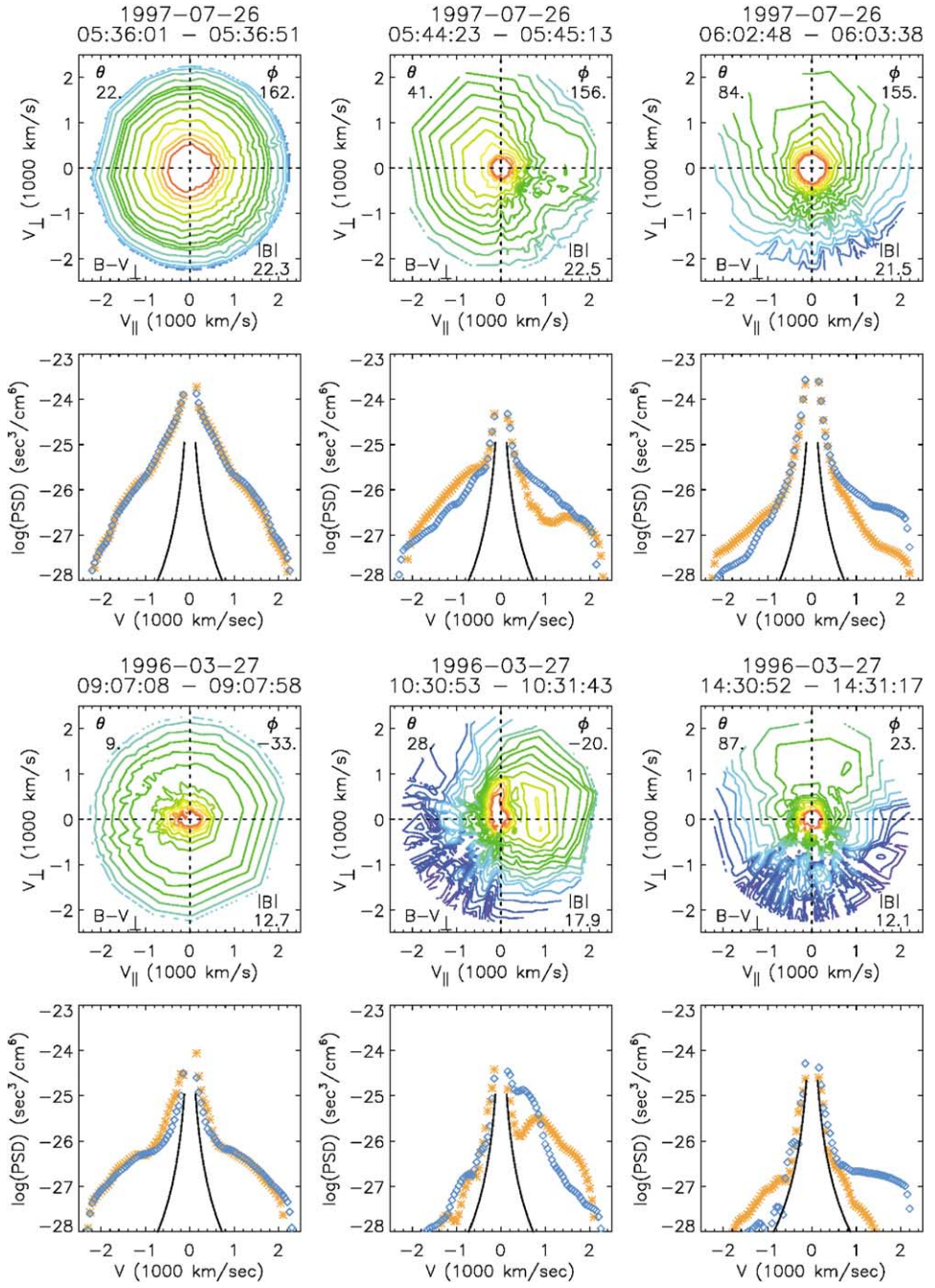

Fig. 4. Examples of the distribution function during two pseudo-breakup and expansion types of aurora. The first and third rows are isocontours of ion velocity distributions in the B–$V_\perp$ plane in the spacecraft frame. The second and fourth rows are cuts of the distribution functions in the direction parallel (orange stars) and perpendicular (blue diamonds) to the magnetic field. The smooth solid line represents the instrument noise level. The left panel represents distributions before large $\langle \mathbf{v} \rangle$ events were observed.

counts averaged over ≈50 s for the July 26, 1997 event and 48 and 24 s for the 1031 and 1430 UT events, respectively, on March 27, 1996.

The distributions before the time of high $\langle \mathbf{v} \rangle$s show nearly circular contours, indicating the ions were generally isotropic. The closer spacing of contours observed on July

26, 1997 than those from March 26, 1996 can be interpreted to mean the plasma distribution had a lower temperature assuming the plasma was in thermal equilibrium. The quiet distributions on March 27, 1996 consisted of two populations, the low energy core and the more energetic plasmas. There is a small anisotropy for the ions travelling along the magnetic field direction, with a larger number from the earthward direction. These are superposed on the higher energy isotropic ions.

While the detailed features of the distributions of ions during high $\langle \mathbf{v} \rangle$ events look different for July 26, 1997 and March 27, 1996, similar phase space features are observed on both occasions. For example, the phase space density on both days is distributed asymmetrically and sharp gradients are observed. The 1031 UT distribution on March 27, 1996 shows a core of low velocity (energy) ions that is anisotropic along the $\mathbf{V}_\perp$ direction and a broad beam ($\approx 45^\circ$) is observed at higher positive velocities ($\approx$900 km/s$\approx$5 keV) centered about the magnetic field direction. The ion beam on March 27, 1966 at 1030:53 UT is travelling along the direction of **B** and given the 28° magnetic elevation angle, the particles in the beam contribute to the mean velocity in the earthward direction. The large mean velocity ($\langle \mathbf{v} \rangle$600 km/s) arises because the phase space density in the other direction is depleted. Note the beam and the core are displaced from the origin along the $+V_\perp$, indicating the plasmas were being $\mathbf{E} \times \mathbf{B}$ convected at $\approx$200 km/s, which accounts for about a third of the total $\langle \mathbf{v} \rangle$ of $\approx$600 km/s. Plasma distributions with clear evidence of $\mathbf{E} \times \mathbf{B}$ are rarely observed. The example shown here is an exception.

Similarly, complex features are observed for the 0544 UT distribution on July 26, 1997 except the phase space density was dominated mainly by the energetic plasma instead of the beam. The distribution is complex as the 1D distribution shows a weak beam travelling in the tailward direction while the calculated $\langle \mathbf{v} \rangle \approx 300$ km/s is in the earthward direction. This earthward $\langle \mathbf{v} \rangle$ is due to the enhancement of the energetic particles that are seen on the left quadrants of the 2D distributions. This period involved complex and multi-component ion distribution and illustrates on rare occasions $\langle \mathbf{v} \rangle$ points in the opposite direction as the beam.

The 0603 and 1431 UT distributions from July 26, 1997 and March 27, 1996 taken from a later period associated with large $\langle \mathbf{v} \rangle$s again show the plasmas were dynamic. The phase space densities remained asymmetric and featured sharp gradients. For both distributions, two populations of ions are evident. This is most clearly seen in the 1D cuts which show the low energy nearly isotropic component (up to $\approx$2 keV) and the asymmetric high energy component (up to $\approx$27 keV). Note the sharp discontinuity in the 1D cut on March 27, 1996 distribution at $\approx$500 km/s. An extremely energetic component extends to the highest energy of our detector. Chen et al. (2000a) has shown that this energetic component extended to 1 MeV. The final point to note is that the energetic broad beams are now observed centered roughly along the $V_\perp$-direction. Like those observed earlier, these energetic ions appear only in one direction while they are depleted in the other direction. As stated earlier, it is this difference in the two directions that contributes in a major way to the calculation of the velocity moments resulting in high $\langle \mathbf{v} \rangle$ values.

3. Discussion

This article has summarized the important results we have recently obtained on the connection between the aurora and the plasma sheet dynamics. Our study, which uses the distribution function as the primary data product, has identified the cause and reason for the large mean velocities ($\langle \mathbf{v} \rangle \geqslant 400$ km/s) frequently observed in the plasma sheet. Detailed distribution functions show that the high values of $\langle \mathbf{v} \rangle$ come from non-uniform phase space features that include non-gyrotropic beams consisting of newly accelerated energetic ions with typical energies of $\approx$10 keV but significant fluxes are observed up to MeV energies. The energy spectra have strong directional dependence with a large gradient in the tailward direction for observations made at tail distances of $\approx 10 R_E$ to $\approx 30 R_E$. Chen et al. (2000a) have shown that the energy spectra of these freshly accelerated ions cannot be produced from an initial isotropic spectra transformed to a Galilean frame of reference, for example, the $\mathbf{E} \times \mathbf{B}$ frame. Only a small number of the observed high $\langle \mathbf{v} \rangle$ events include $\mathbf{E} \times \mathbf{B}$ flows. Even then, the convective flow is usually only a fraction of the total $\langle \mathbf{v} \rangle$. The largest component is usually along the magnetic field direction and it is produced by a dynamic phase space distribution.

These findings indicate that kinetic physics is important for studying plasma sheet and substorm dynamics (Parks et al., 2001). Characterizing the plasma sheet dynamics using only the moments of the distribution function is physically meaningful when the moments are calculated from plasma distributions that consist of a single population and when such distributions are stable in some frame of reference. Macroscopic plasma theory can then be used to describe the dynamics of phenomena that occur at time scales slower than the ion gyro-period. However, the ion distributions in the plasma sheet often include several populations from different sources (Chen et al., 2000b). In addition, a significant variation of **B** occurs close to the local cyclotron frequency, a domain where the fluid description is not valid.

The dynamic features shown above characterize ion distributions of both small-pseudo-breakup and large-scale expansive auroras. This behavior is true for other correlated events we have studied which include more than 50 different cases (not shown). The same ion features are observed during both disturbed and quiet solar wind conditions, when the B_z component of the IMF is northward and southward, and at all phases of a substorm, growth, onset and recovery phases. These findings suggest the same instability process is active for all of the varying size auroras and the disturbance in the plasma sheet, like the aurora, involves a continuum

of intensities and scale sizes. This instability is highly nonlinear as the accompanying magnetic variations have very large amplitudes ($\Delta B/B > 1$).

These observations suggest that a pseudo-breakup aurora is not different from an expansive aurora. A pseudo-breakup aurora expands in latitude like the expansive aurora, albeit the expansion is limited. But it does expand. A pseudo-breakup aurora is also associated with the same kind of large magnetic field fluctuations in the plasma sheet and Pi-2 pulsations on the ground as in an expansive aurora. The amount of energy deposited in a pseudo-breakup aurora is smaller but this energy comes from the same plasma sheet energy. We, therefore, suggest that a pseudo-breakup aurora is produced by the same mechanism that produces an expansive aurora. Both are consequences of substorms except a pseudo-breakup aurora is the consequence of a small substorm and a small region is active in the plasma sheet. A final comment to note is that auroral intensification is due to electrons whereas large $\langle \mathbf{v} \rangle$ events come from energetic ions. Thus, if the two are causally related, some intermediate physical process is needed to convert energy from the large $\langle \mathbf{v} \rangle$ carried by ions or the magnetic field fluctuations into precipitating electrons.

A similar conclusion was reached by Nakamura et al. (1994) and Rostoker (1998) on the causal relationship between the pseudo-breakup and expansive type auroras. Nakamura et al. (1994) used data from ground-based magnetometers, all sky cameras and geosynchronous magnetic field and particle data and concluded that in spite of the difference between a pseudo-breakup and a major expansion onset in their scale size, there seems to be no difference in the physical process. Rostoker (1998) used ground-based magnetometers and photometers and solar wind data and suggest that the physical process responsible for one of the auroral activations during a substorm expansive phase was similar to the pseudo-breakup event.

The auroral brightenings in the pseudo-breakup events on July 26, 1997 start at lower latitude and expand poleward (Figs. 1 and 2) and thus they are not the poleward boundary intensification (PBI) events that Lyons et al. (1999) studied. The PBI brightenings begin at high latitudes, $> 75^\circ$, and move equatorward, reaching the equatorward edge of the oval in 10–20 min. Lyons et al. (1999) suggest that the PBIs are the auroral signatures of bursty bulk flows and they are different auroral phenomenon than the substorm onsets. Their plasma data come from Geotail at larger distance ($\approx 30 R_E$). The large $\langle \mathbf{v} \rangle$ events (identified as bursty bulk flow events) that Wind observed come from a tail distance of $\approx 11 R_E$ and they are associated with Pi-2 emissions and enhancement of auroral kilometric radiation that are identical to ones observed at the substorm expansion onset.

If pseudo-breakup and expansive auroras are both consequences of a substorm different only in the disturbance level, then a different concept about how substorms work emerges. Examples of pseudo-breakup auroras from July 26, 1997 indicate a growth phase (McPherron, 1970) is not needed to trigger a substorm. The growth phase is associated with enhanced convection caused by the more efficient coupling between the solar wind and the magnetosphere and plasma energy increases in the plasma sheet. This increase of plasma energy is needed and will enhance the chances of producing a substorm but it alone does not establish the condition for triggering the substorm instability. Triggering a substorm depends on a number of factors that occur after the energy has been transported into the plasma sheet. We can describe the phenomenology of how the plasma becomes unstable even though the substorm instability has not been identified.

Consider a plasma distribution that is initially in equilibrium in an inhomogeneous medium such as the plasma sheet. Let this plasma be acted on by gradient, curvature and time-dependent electromagnetic forces. These forces will transport the plasma into different regions of the plasma sheet and the original distribution will be modified and become more complex. As the plasma continually evolves in space and time, a non-equilibrium component can develop locally that contributes to free energy. This will permit a considerable amount of free energy to be built up in selected regions of the plasma sheet and a host of instabilities can tap on this energy reservoir. How much free energy and over what regions this free energy develops determines the total energy dissipated and the size and intensity of auroras. Local properties of the ambient plasma distributions are important in determining what instability criteria are satisfied and whether instability should occur.

The picture of plasma sheet dynamics described above is deduced from phase space distributions with time resolutions of 24 and 48 s and spin averaged (3 s) magnetic field data correlated to $\approx$37 s averages of UVI images. A segment of plasma and magnetic field data on July 26, 1997 was, however, obtained with time resolutions of 3 s for the ion phase space distributions and 0.046 s for the magnetic field (burst-mode data). Preliminary analysis of these high time resolution data shows significant phase space variations occur over 3 s and **B** variations are observed up to and beyond the local cyclotron frequency (Fillingim et al., 2002). Magnetic field variations close to the ion cyclotron frequency corroborate the observations of the complex phase space distributions that indicate kinetic physics is important in the instability mechanism. This kind of rapid magnetic field variations has been observed during substorms at geomagnetic tail distances of $\approx 8 R_E$ (Lui, 1991, 1996).

Plasma sheet studies of the dynamics using ion distributions averaged over times longer than the ion cyclotron frequency provide a time "average" picture of what is taking place. To shed light on the details of the substorm instability mechanism would require higher time resolution data. Future publications will address the behavior of high time variations of ions and electrons to provide an even more detailed picture of the plasma sheet dynamics and the substorm mechanism.

Acknowledgements

The research at the University of Washington is supported in part by NASA Grants NAG5-3170 and NAG5-26580 and at the University of California Berkeley by NASA Grant NAG5-2815.

References

Akasofu, S.I., 1964. The development of the auroral substorm. Planetary Space Science 12, 273–282.

Angelopoulos, V., Phan, D.E., Larsen, D.E., Mozer, F.S., Lin, R.P., Tsuruda, K., et al., 1997. Magnetotail flow bursts: association to global magnetospheric circulation, relationship to ionospheric activity and direct evidence for localization. Geophysical Research Letters 24, 2271.

Baumjohann, W., Paschmann, G., Luhr, H., 1990. Characteristics of high-speed ion flows in the plasma sheet. Journal of Geophysical Research 95, 3801.

Chen, L.-J., Parks, G.K., McCarthy, M., Larson, D., Lin, R.P., 2000a. Kinetic properties of bursty bulk flow events. Geophysical Research Letters 27, 1847.

Chen, L.-J., Larson, D., Lin, R.P., McCarthy, M., Parks, G., 2000b. Multicomponent plasma distributions in the tail current sheet associated with substorms. Geophysical Research Letters 27, 843.

Elvey, C.T., 1957. Problems of auroral morphology. Proceedings of the National Academy of Sciences, Washington 43, 63.

Fairfield, D.H., Mukai, T., Brittnacher, M., Reeves, G.D., Kokobun, S., Parus, G.K., et al., 1999. Earthward flow bursts in the inner magnetotail and their relation to auroral brightenings, AKR intensification, geosynchronous particle injections and magnetic activity. Journal of Geophysical Research 104, 355.

Fillingim, M.O., Parks, G.K., Chen, L.J., Brittnacher, M., Germany, G.A., Spann, J.F., Larson, D., Lin, R.P., 2000. Coincident POLAR/UVI and WIND observations of pseudobreakups. Geophysical Research Letters 27, 1379.

Fillingim, M.O., Parks, G.K., Chen, L.J., McCarthy, M., Spann, J.F., Lin, R.P., 2001a. Comparison of Plasma sheet dynamics during pseudobreakups and expansive aurorae, Physics of Plasmas 8, 1127.

Fillingim, M.O., Parks, G.K., Chen, L.J., Larson, D., Lin, R.P., McCarthy, M., 2002. Characterizing plasma sheet dynamics using 3 s ion distribution functions and 0.046 s magnetic field data. In: Sharma, S. (Ed.), Geophysical Monograph, American Geophysical Union, Washington D.C. (to appear).

Lin, R.P., Anderson, K.A., Ashford, S., Carlson, C., Curtis, D., Ergun, D., et al., 1995. A three-dimensional plasma and energetic particle investigation for the Sind spacecraft. Space Science Review 71, 125.

Lui, A.T.Y., 1991. Extended consideration of a synthesis model for magnetospheric substorms. In: Kan, J.R., Potemra, T.A., Kokubun, S., and Iijima, T. (Eds.), Magnetospheric Substorms. Geophysical Monograph 64, American Geophysical Union, Washington, DC.

Lui, A.T.Y., 1996. Current disruption in the earth's magnetosphere: observations and models. Journal of Geophysical Research 101, 12,067.

Lyons, L.R., Nagai, T., Blanchard, G.T., Samson, J.C., Yamamoto, T., Mukai, T., Nishida, A., Kokubun, S., 1999. Association between Geotail plasma flows and auroral poleward boundary intensifications observed by CANOPUS photometers. Journal of Geophysical Research 3, 4485.

McPherron, R.L., 1970. Growth phase of magnetospheric substorms. Journal of Geophysical Research 75, 5592.

Nakamura, R., Baker, D.N., Yamamoto, T., Bellian, R.D., Bering, E.A., Benbrook, J.R., Theal, J.R., 1994. Particle and field signatures during pseudo-breakup and major expansion onset. Journal of Geophysical Research 99, 207.

Parks, G.K., Chen, L.J., Fillingim, M., McCarthy, M., 2001. Kinetic characterization of plasma sheet dynamics. Space Science Review 95, 237.

Rostoker, G., 1998. On the place of the pseudo-breakup in a magnetospheric substorm. Geophysical Research Letters 25, 217.

Torr, M., et al., 1995. A far ultraviolet imager for the International Solar Terrestrial Physics Mission. Space Science Review 71, 329.

Tsyganenko, N.A., 1989. A magnetospheric magnetic field model with a warped tail current sheet. Planetary Space Science 37, 5.